Research Article

A New Strategy for the Preparation of Porous Silk Fibroin Scaffolds

Zhang T[1,2], Xiong Q[2], Shan Y[1]* and Zhang F[3]

[1]Department of Urology, The Second Affiliated Hospital of Soochow University, Suzhou, Jiangsu, China

[2]Department of Urology, Children's Hospital of Soochow University, Suzhou, Jiangsu, China

[3]College of Textile and Clothing Engineering, National Engineering Laboratory for Modern Silk, China

*Corresponding author: Yuxi Shan, Department of Urology, The Second Affiliated Hospital of Soochow University, Suzhou, Jiangsu, China

Abstract

In order to prepare Silk Fibroin (SF) scaffolds with excellent pore structure, the fresh SF solution was concentrated at relative humidity 55% and 25ºC for 3 days. During the above process, SF micelles, existed in the fresh SF solution, aggregated into nanofilaments as concentration increased, and the nanofilament feature of SF were similar to that observed in silk gland. SF nanofilaments were easy to form SF scaffolds with porous and silk I structure, in contrary, SF micelles were liable for formation of SF scaffolds with lamellar and random coil structure. It suggested that the formation of SF nanofilaments is a critical step for pore and secondary structure control of lyophilized SF scaffolds.

Keywords: Silk fibroin; Porous materials; Microstructure; Nanofilaments

Introduction

Silk is a unique material, which has historically been regarded as high-grade raw materials of textile for its strength and luster [1]. Silk-based materials have been transformed from the commodity textile to a growing web of applications in high-technology areas, especially as a biomaterial because of several desirable properties [2]. In particular, these properties include its biocompatibility, biodegradation, and versatility in processing into multiple materials formats [1]. The porous SF scaffolds have attracted considerable attention because it can provide a versatile 3D porous structure which is known to play a critical role for cell attachment, proliferation, migration, and tissue growth, as well as for nutrient and waste transport [3].

Porous SF scaffolds can be fabricated by a variety of methods, including lyophilization, porogens, gas foaming, etc. [1]. However, the scaffolds from pure SF solution undergo lyophilization easily form separate layers or lamellar structures rather than porous structures, and this lamellar structure will cause the loss of compressive properties and affect its application as a biomaterial [4,5]. Recently, it is reported that the porous structure of lyophilized SF scaffolds was closely related to SF assembly nanostructure. SF scaffolds with excellent pore structure could be prepared from nanofilament solution which derived from concentrated SF solution [6]. However, the way used to control drying rate of SF solution by a series of lids with hole is unstable due to the change of temperature and relative humidity around [7]. In our previous research, it was found that temperature and relative humidity played an important role in controlling SF self-assembly and the secondary structure of regenerated SF films [7,8].

In this paper, we firstly prepared SF solution with nanofilaments through controlling concentrating conditions of temperature and relative humidity. Subsequently, the effect of SF nanostructure on morphology, structure and thermal property of porous SF scaffolds was investigated in detail.

Material and Methods

Preparation of *B. mori* SF nanofilaments solution

SF aqueous solution was prepared as described previously [9].

The aqueous SF solution was concentrated in Binder Temperature & Humidity Chamber (Binder, German) at relative humidity 55% and temperature 25ºC for 3 days. The final concentration was ~25 wt%, determined by weighing the remaining solid after drying.

Preparation of SF scaffold

The fresh and concentrated SF solution were diluted to 2%, and then were placed at -20ºC for 24 h to freeze and then lyophilized for 72 h.

Characterization

The morphology of SF in water was observed by AFM (Veeco, Nanoscope V) in air. A 225μm long silicon cantilever with a spring constant of 3 Nm-1 was used in tapping mode at 0.5-1 Hz scan rate.

The morphology of SF scaffolds was observed using SEM (Hitachi S-520, Japan) at 20ºC, 60 RH. Samples were mounted on a copper plate and sputter-coated with gold layer 20-30 nm thick prior to imaging.

The structure of the scaffolds was analyzed by FTIR on a Magna spectrometer (NicoLET5700, America), X-ray diffractometer (X'Pert-Pro MPD, PANalytical B.V. Holland),

Thermogravimetry/differential thermal analysis (TG-DTA, PE-S', America), and TA instrument Q100 DSC (TA instruments, New Castle, DE).

Results and Discussion

It is well known that pore architecture in scaffolds plays a critical role in tissue engineering for the seeded cells to form goal tissue and organs [10]. The morphology of SF in solution and porous 3D scaffolds was examined by AFM and SEM. The fresh SF solution showed a micelle structure, as Figure 1a showed, and the scaffolds from this solution showed separate layer or lamellar structure rather than porous 3D structure as our previous report (Figure 2a,2b) [5]. SF nanofilaments were formed at relative humidity 55% and 30ºC for 3 days as the concentration increased, as Figure 1b showed, and the nanofilament features of SF were similar to this observed
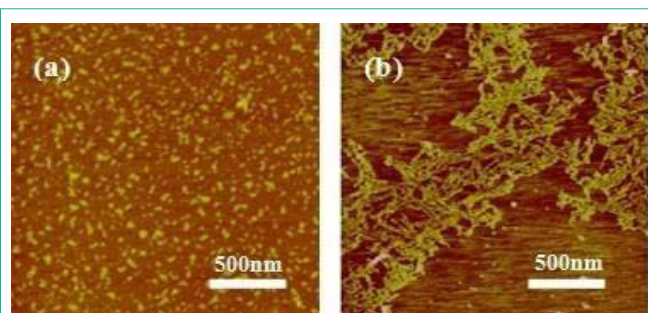
Figure 1: AFM images of SF in solution with concentration of: 0.0001%. (a) The fresh SF solution; (b) The solution was treated by slowly concentrating process; (c) The SF solution isolated from the middle gland of matured 5th *B. mori* silkworm larvae.
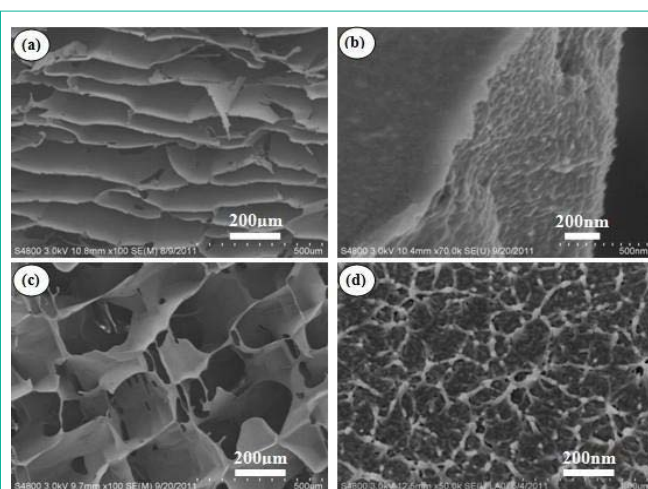

Figure 2: SEM photography of the porous SF scaffolds prepared from fresh SF solution (a) and (b); concentrated SF solution (c) and (d). Each sample is shown in two scales.
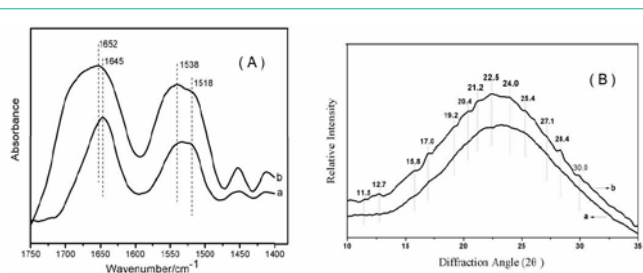

Figure 3: FT-IR spectra (A) and XRD data (B) of porous SF scaffolds prepared from (a) fresh SF solution; (b) concentrated SF solution.
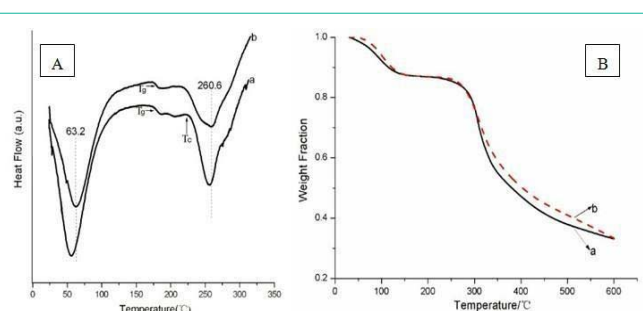

Figure 4: Standard DSC (A) and TGA curves (B) of porous SF scaffolds prepared from (a) fresh SF solution; (b) concentrated SF solution.

in the silk gland [11]. The scaffolds derived from above solution containing SF nanofilament demonstrated excellent porous structure, as Figure 2c showed. It had been also reported that lyophilized SF scaffolds with excellent porous structure which were prepared from SF isolated from silk glands [10], indicating the important role of bionic nanofilament structure in the formation of porous structure. Furthermore, the micelle and nanofilament structure of SF observed in fresh and concentrating solution were also found in the cross-section of relevant SF scaffolds (Figure 2b,2c). The nanofilament, similar to ECM structure, in porous SF scaffolds would provide a favorable microenvironment for cells growth and proliferation [6].

To investigate conformational changes of SF scaffolds derived from different nanostructure solution, FTIR structural analysis was performed (Figure 3a). The peaks at 1610-1630 cm^{-1} and 1510-1520 cm^{-1} were characteristic of silk II conformation, and the absorptions at 1648-1654 cm^{-1} and 1535-1542 cm^{-1} were correspond to silk I structure [12,13]. The scaffolds prepared with fresh SF solution (micelle) showed a strong absorption peak at 1645 cm^{-1} and 1532 cm^{-1}, corresponding to random coil, and a shoulder peak at 1518 cm^{-1}, as shown in Figure 3a. When scaffold was formed from concentrated SF solution (nanofilament) exhibited strong absorption peak at 1652 cm^{-1} and 1538 cm^{-1} (silk I), and the shoulder peak at 1518 cm^{-1} (silk II)

decreased compared to sample a, as shown in Figure 3a.

Besides FTIR, the structure changes of porous SF scaffolds were also confirmed by XRD analysis. Figure 3b showed the XRD data of the SF scaffolds prepared from fresh solution (a) and concentrated solution (b). The two scaffolds showed an amorphous structure, characterized by the presence of a broad peak in the 2θ scattering angle range from 10 to 35°. However, compared with sample a, sample b showed diffraction peaks at 2θ values of 11.5(I), 12.7(II), 19.2(I), 20.4(I), 22.5(I), 24.0(II), 25.4(I), 28.4(I), 30.0(I), indicating the formation of silk I and silk II structure, especially the formation of silk I structure [7]. The XRD results were consistent with the FTIR results, confirming the formation of silk I structure through lyophilizing the frozen concentrated SF solution. Water-insoluble silk films with silk I structure instead of random structure have been prepared by controlling the dry rate of fresh SF solution [7]. In the present study, porous SF scaffolds with partial silk I structure were prepared by concentrated SF solution.

The thermal properties of the dried SF scaffolds were also examined by standard Differential Scanning Calorimetry (DSC) and Thermal Gravimetric Analysis (TGA). Figure 4a illustrated standard DSC curves for SF scaffolds prepared from fresh (sample a) and concentrated (sample b) SF solution. Sample a showed an endothermic peak at 56°C, an obvious glass transition Temperature (Tg) at around 180°C, a non-isothermal crystallization peak appeared around 230°C, and a degradation peak at 257°C. The endothermic peak at 56°C was due to the evaporation of bound water. The glass transition temperature regions of sample a was similar to previous report [14]. After the glass transition temperature regions, an obvious nonisothermal crystallization peak at 230°C is related to the thermal transition of SF molecular from unstable non-crystal structure to crystal structure [15]. Finally, sample a started to degrade with

endothermic peak at around 257°C.

Sample b showed a Tg at around 180°C which was similar to sample a, but the crystallization peak disappeared because of the formation of silk I crystals which had been confirmed above by FTIR and XRD. The disappear of crystallization peak indicated that silk I was a stable structure under degradation peak at around 260°C. The endothermic peak of water inside SF scaffolds and degradation peak increased to 63.2 and 260.6°C, which were likely due to the silk I structure formed during the concentrated process and the silk I crystal is a hydrated structure [7].

The TGA results confirmed that stronger water-silk interactions and more stable thermal property due to the increase of silk I content formed during concentrated process, though the weight loss was same when the temperature reached 120°C and 600°C, as Figure 4b showed.

Conclusions

In this paper, we prepared SF scaffolds with 3D porous structure by controlling the SF assembly. Under relative humidity 55% and 30°C, SF assembled nanofilaments after 2 days with the concentration increase from about 2 wt% to 30 wt%. SF scaffolds derived from nanofilament solution demonstrated porous and silk I structure, in contrary, SF scaffolds derived from micelles solution showed layered and random coil structure, suggesting that the biotic structure of SF nanofilament is a key parameter for controlling the morphology and structure of regenerated SF scaffolds. SF scaffolds with porous structure would further facilitate the use of SF in tissue engineering.

Acknowledgement

References

1. Rockwood DN, Preda RC, Yucel T, Wang X, Lovett ML, Kaplan DL. Rockwood DN, Preda RC, Yucel T, Wang X, Lovett ML, Kaplan DL. Nat Protoc. 2011; 6: 1612-1631. Nat Protoc. 2011; 6: 1612-1631.

2. Omenetto FG, Kaplan DL. Science. New Opportunities for an Ancient Material. 2010; 329: 528-531.

3. Vepari C, Kaplan DL. Prog Polym Sci. Silk as a Biomaterial. 2007; 32: 991-1007.

4. Lv Q, Feng Q, Hu K, Cui F. Polymer. Three-dimensional fibroin/collagen scaffolds derived from aqueous solution and the use for HepG2 culture. 2005; 46: 12662-12669.

5. Lu Q, Zhang X, Hu X, Kaplan DL. Macromol Biosci. Green process to prepare silk fibroin/gelatin biomaterial scaffolds. 2010; 10: 289-298.

6. Lu Q, Wang X, Lu S, Li M, Kaplan DL, Zhu H. Nanofibrous architecture of silk fibroin scaffolds prepared with a mild self-assembly process. Biomaterials. 2011; 32: 1059-1067.

7. Lu Q, Hu X, Wang X, Kluge JA, Lu S, Cebe P, et al. Water-insoluble silk films with silk I structure. Acta Biomater. 2010; 6: 1380-1387.

8. Ming J, Zuo B. Silk I structure formation through silk fibroin self-assembly. J Appl Polym Sci. 2012; 125: 2148-2154.

9. Zhang F, Zuo B, Fan Z, Xie Z, Lu Q, Zhang X, et al. Mechanisms and control of silk-based electrospinning. Biomacromolecules. 2012; 13: 798-804.

10. Mandal BB, Kundu SC. Cell proliferation and migration in silk fibroin 3D scaffolds. Biomaterials. 2009; 30: 2956-2965.

11. Lu Q, Zhu H, Zhang C, Zhang F, Zhang B, Kaplan DL. Silk Self-Assembly Mechanisms and Control From Thermodynamics to Kinetics. Biomacromolecules. 2012; 13: 826-832.

12. Hu X, Shmelev K, Sun L, Gil ES, Park SH, Cebe P, et al. Regulation of silk material structure by temperature-controlled water vapor annealing. Biomacromolecules. 2011; 12: 1686-1696.

13. Jin HJ, Park J, Karageorgiou V, Kim UJ, Valluzzi R, Cebe P, et al. Adv Funct Mater. 2005; 15: 1241-1247.

14. Hu X, Kaplan DL, Cebe P. Dynamic Protein-Water Relationships during β-Sheet Formation. Macromolecules. 2008; 41: 3939-3948.

15. Hu X, Lu Q, Sun L, Cebe P, Wang X, Zhang X, et al. Biomacromolecules. 2019.